Available online at www.sciencedirect.com
ScienceDirect
Journal of Catalysis 245 (2007) 401–414
JOURNAL OF CATALYSIS
www.elsevier.com/locate/jcat

Characterisation and microstructure of Pd and bimetallic Pd–Pt catalysts during methane oxidation

Katarina Persson [a,*], Kjell Jansson [b], Sven G. Järås [a]

[a] *Chemical Technology, Department of Chemical Engineering and Technology, KTH, Teknikringen 42, SE-100 44, Stockholm, Sweden*
[b] *Arrhenius Laboratory, Department of Inorganic Chemistry, University of Stockholm, S. Arrhenius väg 12, SE-106 91 Stockholm, Sweden*

Received 15 September 2006; revised 25 October 2006; accepted 28 October 2006

Available online 30 November 2006

Abstract

The catalytic oxidation of methane was studied over Pd/Al_2O_3 and $Pd–Pt/Al_2O_3$. It was found that the activity of Pd/Al_2O_3 gradually decreases with time at temperatures well below that of PdO decomposition. The opposite was observed for $Pd–Pt/Al_2O_3$, of which the activity decreases slightly with time. Morphological studies of the two catalysts showed major changes during operation. The palladium particles in Pd/Al_2O_3 are initially composed of smaller, randomly oriented crystals of both PdO and Pd. In oxidising atmospheres, the crystals become more oxidised and form larger crystals. The activity increase of $Pd–Pt/Al_2O_3$ is probably related to more PdO being formed during operation. The particles in $Pd–Pt/Al_2O_3$ are split into two different domains: one with PdO and the other likely consisting of an alloy between Pd and Pt. The alloy is initially rich in palladium, but the composition changes to a more equalmolar Pd–Pt structure during operation. The ejected Pd is oxidised into PdO, which is more active than its metallic phase. The amount of PdO formed depends on the oxidation time and temperature.

Keywords: Palladium; Platinum; Bimetal; Methane; TEM; PXRD; TPO; XPS; Stability; Catalytic combustion

1. Introduction

Catalytic oxidation of methane under oxygen-rich conditions has received considerable attention. One of the reasons is the increasing interest in lean-burn natural gas vehicles (NGVs). Compared with diesel engines, NGV engines produce less NO_x and particulates [1–3]. However, a problem with NGV engines is the high level of unburned methane in the exhaust. Because methane is a potent greenhouse gas, it is important to reduce the amount emitted into the atmosphere. One approach to abating methane emission is the use of catalytic exhaust converters, in which the abatement is achieved by catalytic oxidation.

Another application for catalytic oxidation of methane is in catalytic gas turbine combustors [4,5]. Instead of combusting the fuel homogeneously using a flame, the fuel is combusted over catalysts. In this way, the combustion temperature is considerably reduced, and the formation of thermal NO_x is decreased. Natural gas is a frequently used fuel in gas turbines, and the major combustible component in natural gas is methane.

A catalyst that often has been used for these applications is palladium supported on various washcoats [6,7]. Many studies have shown that the activity over fresh palladium catalysts is excellent for methane oxidation under lean conditions. However, it has recently been reported that palladium-supported catalysts have poor stability for methane conversion when the temperature is kept constant [8–13]. The initially high activity when the catalysts are fresh drops significantly during operation, resulting in increasing difficulty in igniting the methane at desirable temperatures.

Different additives may be used to improve the palladium catalyst. One of the more promising additives is Pt, which considerably improves the stability during reaction [8,9,11,14]. Recent results from our lab have shown even a slight increase in the activity for the Pd–Pt catalysts with time [11,15]. A considerable number of papers have also shown that the activity of the bimetallic Pd–Pt catalysts is improved in comparison to

* Corresponding author. Fax: +46 8 108579.
E-mail address: katarina.persson@ket.kth.se (K. Persson).

0021-9517/$ – see front matter
doi:10.1016/j.jcat.2006.10.029

the monometallic palladium catalysts [8,16–18]. These properties make the bimetallic Pd–Pt catalysts more attractive than the monometallic palladium catalysts.

In this work, the combustion behaviour during methane oxidation is correlated to morphologic changes of the catalyst on various treatments. To investigate the reason for the decrease or increase in activity for the monometallic palladium catalyst and the bimetallic Pd–Pt catalyst, respectively, various temperature-programmed oxidation analyses were carried out. The samples were also studied by TEM, EDS, PXRD, and XPS. Furthermore, the thermal aging properties were evaluated for both the monometallic and bimetallic catalysts.

2. Experimental

2.1. Catalyst preparation

A palladium catalyst and a palladium–platinum catalyst, both supported on γ-Al_2O_3 (PURALOX HP-14/150, Sasol Germany GmbH), were investigated in this study. The two catalysts were prepared so as to have equal loadings of noble metals (470 μmol metal/g catalyst powder). The molar ratio between Pd and Pt in the bimetallic catalyst was 2:1. More details on the catalysts are given in Table 1.

The alumina powder was impregnated with the metal/metals by the incipient wetness technique. Solutions of palladium (Johnson Matthey) and platinum nitrate (Kaabs Materials AB) were mixed with deionised water before impregnation. The support was impregnated twice, with a drying step at 300 °C for 4 h between steps, and calcined at 1000 °C for 1 h.

The catalyst powders were mixed with ethanol before ball milling. Cordierite monoliths (400 cpsi, Corning), with ∅14 mm and length 10 mm, were then dip-coated in the slurry, followed by a drying step at 100 °C. This procedure was repeated until 20 wt% of catalyst material was fastened onto the monolith. Finally, the coated monoliths were calcined at 1000 °C for 2 h.

2.2. Activity tests

Catalytic activity measurements were carried out at atmospheric pressure using a tubular reactor placed inside a programmable furnace. A gas mixture of 1.5 vol% CH_4 in air was fed to the reactor at a space velocity of 250 000 h^{-1} for all types of activity tests. The temperature of the gas was recorded by a thermocouple placed upstream of the monolith. The reaction products were analysed on-line by gas chromatography (GC Varian 3800), equipped with a thermal conductivity detector.

Two different activity tests were performed for the as-prepared catalysts. In the first test, the catalyst was studied for 12 h with the temperature maintained at 500 °C. In the second test, the temperature was varied among 500, 550, and 600 °C, with each temperature maintained for 30 min. A new sample was used for each experiment.

2.3. Characterisation

Inductively coupled plasma–atomic emission spectroscopy (ICP-AES) was performed on the catalysts to verify the amounts of palladium and platinum. The specific surface areas of the catalyst powders were measured by nitrogen adsorption at liquid N_2 temperature in a Micromeritics ASAP 2010 instrument. The surface area was determined according to the Brunauer–Emmett–Teller (BET) theory. Before analysis, the samples were degassed for at least 2 h at 250 °C.

The crystal phases in the catalysts were monitored by powder X-ray diffraction (PXRD), using both a Guinier–Hägg camera with a radius of 40 mm and diffractometer (Siemens Diffraktometer D5000). In the former case, Si was added as an internal standard, and the powder X-ray photographs were evaluated by the Scanner System program [19] to obtain the d values. The phases were identified using the JCPD database. The mean crystal sizes were estimated from the diffractometer data using the Fundamental Parameter Approach application of the TOPAS v2.0 software.

The redox properties of the catalysts were analysed by temperature-programmed oxidation (TPO). The experiments were carried out using a Micromeritics AutoChem 2910 equipped with a thermal conductivity detector. As-prepared catalyst powder (100 mg) was placed on top of glass wool in a quartz reactor, and 5 vol% O_2/He was continuously flowed over the sample at 20 ml/min. The temperature was cycled between 300 and 900 °C at a rate of 10 °C/min. The temperature cycle was repeated twice; the results from the second cycle are presented in this paper, because water desorption affected the first cycle. For most experiments, the sample was preoxidised at various temperatures and for varying durations before the second temperature cycle. A new sample was used for each analysis.

The morphologies and sizes of the noble metal particles on the alumina were studied by transmission electron microscopy (TEM), using a JEOL 2000 FX microscope equipped with an energy-dispersive X-ray spectroscopy (EDXS) detector (LINK AN 10000). Surface analyses of the samples were conducted

Table 1
A summary of the catalysts and their textural properties

Sample	Composition	Pd loading (wt%)	Pt loading (wt%)	BET surface area (m^2/g)	Crystal size[a] PdO (nm)	Crystal size[a] Pd–Pt (nm)
Pd/Al_2O_3	5 wt% Pd/Al_2O_3	5.1	0	102	26	–
Pd/Al_2O_3-aged	5 wt% Pd/Al_2O_3-aged	4.8	0	84	27	–
$PdPt/Al_2O_3$	2:1 $Pd:Pt/Al_2O_3$	3.0	3.3	91	19	34
$PdPt/Al_2O_3$-aged	2:1 $Pd:Pt/Al_2O_3$-aged	3.0	2.8	71	20	33

[a] Estimated by TOPAS—Fundamental Parameter Approach.

with a Shimadzu ESCA 3400 using Mg$K\alpha$ radiation. The samples were fastened onto one side of double-adhesive tape, the other side fastened onto the instrument sample holder. The experiments were performed at a pressure of 10^{-6} Pa using a radiation power of 10 kV and 20 mA. After a scan in the range of 0–600 eV, the energy ranges 62–80 eV (Al2p), 280–300 eV (C1s), 330–350 eV (Pd3d), and 523–544 eV (O1s) were scanned for 12 h. Al 1s was used to correct spectra for charge-up effects, where spectra were corrected to an energy of 74.5 eV. The spectrometer resolution was taken from the C1s spectra, and convolution was performed using all three energy states, 335.2 eV (Pd^0), 336.7 eV (Pd^{2+}), and 337.5 eV (Pd^{4+}), for each sample.

2.4. Thermal aging

Both the catalytic powders and the monoliths were aged for 10 h in a tubular furnace at 1000 °C with a flow of air of 15 vol% of steam. The activity tests were carried out under the same conditions as described in Section 2.2, except for the temperature being increased stepwise from 470 to 770 °C, with each temperature step maintained for 1 h. Both as-prepared and aged monoliths were tested. Before the activity tests, the temperature was increased to 900 °C to stabilise the samples.

3. Results and discussion

3.1. Catalytic activity

The results from the activity measurements over Pd/Al_2O_3 and $PdPt/Al_2O_3$ are shown in Figs. 1 and 2, respectively. The black curves display the activity over 12 h with the inlet temperature to the catalyst maintained at 500 °C. As shown in Fig. 1, the Pd/Al_2O_3 catalyst initially had excellent activity with 53% methane conversion, but the activity dropped rapidly with time. After 12 h, the conversion was only 11%.

In the same figure, the gray dotted curve represents the activity of Pd/Al_2O_3 with the temperature alternated among 500, 550, and 600 °C. It is clear that the deactivation was enhanced at higher temperatures, because the activity already at the third temperature step was lower than the activity measured when the temperature was maintained at 500 °C. The conversion at the end of the test was only 4%, whereas that after the same time for the sample maintained at 500 °C was 14%.

Fig. 2 shows the results of the two activity tests over $PdPt/Al_2O_3$, but in a different range than displayed in Fig. 1. For the 12-h test, the initial activity was lower than its monometallic counterpart, and the activity showed a small drop during the first 50 min. This initially lower activity of the bimetallic catalyst is expected because the amount of palladium in the catalyst was only two-thirds of the amount in Pd/Al_2O_3. In addition, palladium is generally known to have higher activity for methane combustion than platinum [20]. However, the conversion actually increased with time over the remainder of the activity test. The increase levelled out at the end of the test.

The gray dotted curve in Fig. 2 represents the activity over $PdPt/Al_2O_3$ at 500, 550, and 600 °C. The higher-temperature steps appear to enhance the activity slightly at 500 °C, indicating that the temperature is important to the activation process. It is interesting to note that the activity of $PdPt/Al_2O_3$ was actually higher than the activity of Pd/Al_2O_3 after only 6.6 h for the samples maintained at 500 °C; when the temperature was cycled, $PdPt/Al_2O_3$ achieved superior activity more rapidly.

The poor stability of methane conversion over monometallic palladium catalysts has been explained by Narui et al. [8] as a size effect of the Pd particles. Adding platinum to this cata-

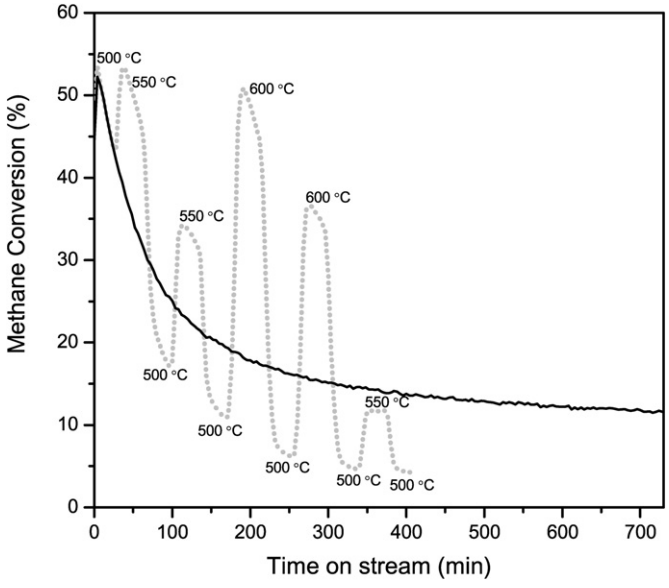

Fig. 1. Methane conversion versus time on stream over Pd/Al_2O_3. The black curve represents the activity of the sample kept at 500 °C and the gray dotted curve represents the activity of the sample at 500, 550 and 600 °C, respectively.

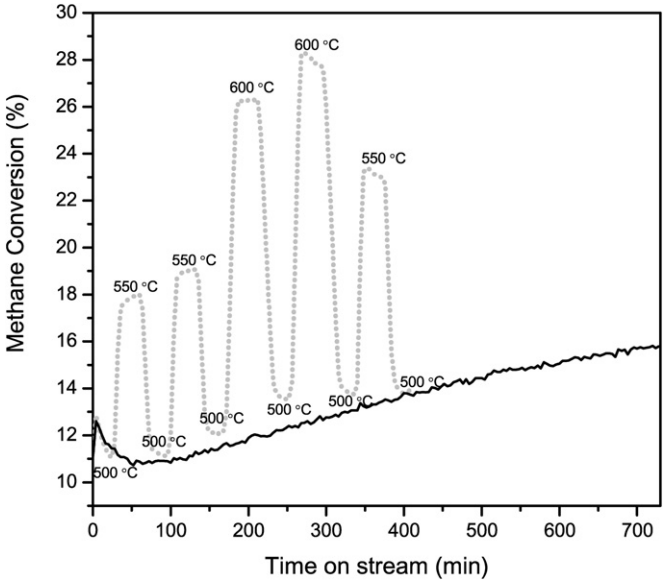

Fig. 2. Methane conversion versus time on stream over $PdPt/Al_2O_3$. The black curve represents the activity of the sample kept at 500 °C and the gray dotted curve represents the activity of the sample at 500, 550 and 600 °C, respectively.

lyst resulted in considerably more stable activity. Their Pd–Pt catalyst showed lower particle growth than its monometallic counterpart. Araya et al. [21] reached a different conclusion, that the loss of dispersion of their Pd-based catalyst was too small to be essential. Their fresh catalyst had a dispersion of 31.7%, and after the catalyst was used for 96 h, the dispersion was 28.2%. Nonetheless, these authors observed a significant drop in activity with time for their Pd-based catalyst.

The poor stability of monometallic Pd catalysts also has been attributed to poisoning by the water produced during oxidation of methane [13,22,23]. The poisoning process has been suggested to be due to formation of $Pd(OH)_2$, which is less active for methane oxidation, resulting in decreased activity. Even though most authors have reported decreased activity when extra water is added to the feed stream, this does not prove that $Pd(OH)_2$ has been formed, especially not at this high temperature, where hydrothermal processes of alumina may occur. Thus, there may be other explanations for deactivation besides $Pd(OH)_2$ formation, for instance, hydrothermal reaction with the support.

3.2. Oxidation for various lengths of time

The changes of the catalysts with time while temperature was held constant at 500 °C have been studied by TPO; the results are shown in Figs. 3 and 4. The catalyst powders were preoxidised at 500 °C before the second TPO cycle. For Pd/Al_2O_3, presented in Fig. 3, two positive peaks occurred during heating. The first, small peak appeared at around 730 °C; the second, larger peak appeared at 790 °C and persisted up to 900 °C. During cooling, a negative peak occurred, starting at 630 °C and ending at 460 °C. The peaks appearing during heating are generally known to be due to oxygen release when PdO decomposes into its metallic state [24,25]. The negative peak during cooling can be attributed to oxidation of metallic Pd back to PdO. The temperature hysteresis between decomposition and reoxidation is a well-known phenomenon in supported palladium catalysts [26,27]. The cause of this hysteresis has been suggested to be an effect of a nucleation mechanism when Pd is reoxidised [7]; however, the literature on this hysteresis phenomenon is diverse.

The decomposition peaks during heating changed with preoxidation. The total area of the decomposition peaks increased slightly with preoxidation, indicating that more PdO was formed during preoxidation. If this is also true under the reaction conditions, then deactivation of Pd/Al_2O_3 may not be due to loss of the PdO phase.

The ratio between the areas of the two decomposition peaks also changes with preoxidation. The first peak became smaller with increasing preoxidation time, whereas the second peak became larger. These results are similar to those of Groppi et al. [25], who explained this behaviour with two different Pd oxide species. The first peak represents one type of oxide, transferred during heating into a second type of PdO, shown as the second peak. However, the origin of these species has not been established. During cooling, the reoxidation peak was not affected by the preoxidation time.

For the as-prepared Pd/Al_2O_3 sample, a broad decrease of the oxygen signal between 450 and 630 °C was observed during heating, indicating that the sample was taking up oxygen from the feed gas. This is probably because the reoxidation of Pd was not completed during the first cooling ramp (not shown in figure), but continues during the second heating ramp. When the sample was preoxidised, the oxygen uptake during the heating ramp disappeared. Thus, the oxidation of Pd proceeded further during the preoxidation step.

The incomplete reoxidation on cooling in the TPO experiment was also suggested by the reoxidation coefficient δ, de-

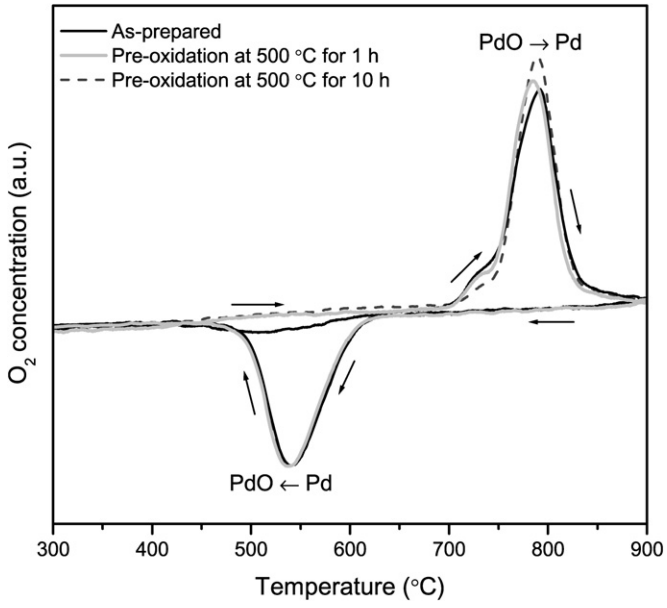

Fig. 3. TPO profiles of Pd/Al_2O_3. The sample was either as-prepared or preoxidised for various lengths of time.

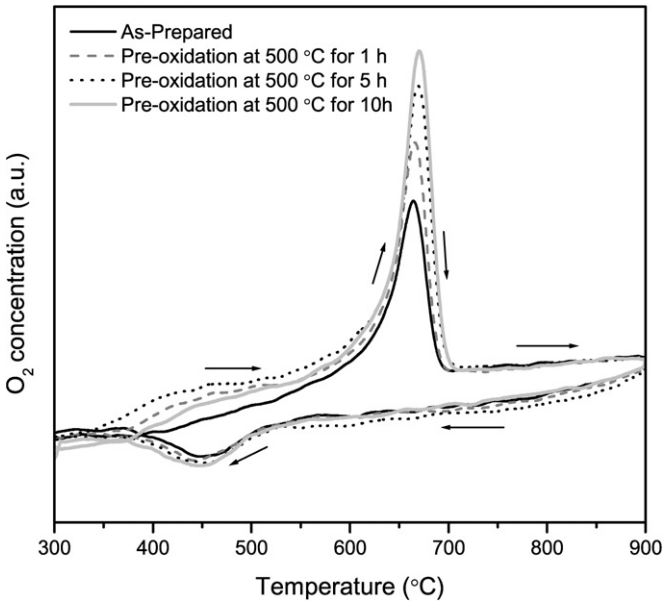

Fig. 4. TPO profiles of $PdPt/Al_2O_3$. The sample was either as-prepared or preoxidised for various lengths of time.

Table 2
The reoxidation coefficient δ of the samples that were preoxidised at 500 °C during various lengths of time

Sample	As-prepared	1 h	5 h	10 h
Pd/Al_2O_3	1.33	1.37	–	1.41
$PdPt/Al_2O_3$	2.43	3.07	4.03	3.88

fined here as the area of the decomposition peaks divided by the area of the reoxidation peak. If the catalyst were to be as oxidised after the cooling ramp as before the decomposition peaks, then δ would be equal to 1; that is, the areas of the decomposition peaks and of the reoxidation peak would be equal. As shown in Table 2, this is not the case for Pd/Al_2O_3, but the value was >1, reflecting incomplete oxidation during cooling. The δ value increased to some extent with increasing preoxidation time. This result was associated more with variations in the area of the decomposition peaks than with variations in the reoxidation peak area.

The TPO profile of the $PdPt/Al_2O_3$ catalyst is shown in Fig. 4 for various preoxidation periods at 500 °C. The reduction peak during heating appears at a lower temperature than for Pd/Al_2O_3, indicating that Pt promotes the reduction of PdO. This is in line with previous reports [9,28]. The temperature at the maximum of the reduction peak was 664 °C for the as-prepared $PdPt/Al_2O_3$ catalyst. By preoxidising the sample, the peak maximum moved to slightly higher temperatures.

The preoxidation time strongly affected the intensity of the reduction peak, considerably more than for the Pd/Al_2O_3 catalyst. The peak intensity of the as-prepared $PdPt/Al_2O_3$ catalyst was significantly lower than that for the sample preoxidised for 1 h. When the sample was preoxidised for 5 h, the peak intensity was even larger. However, the change was smaller between 5 and 10 h of preoxidation. Our previous high-temperature XRD studies [15] showed that the TPO peak during heating was most likely attributable to PdO decomposition, as in the case of the monometallic Pd catalyst. Therefore, the increase in the positive peak during heating presumably was due to increased PdO formation during preoxidation. If this was also the case under reaction conditions, then it was not surprising that the activity increased with time. Previous studies at our laboratory showed that the Pd–Pt alloy itself has poor activity for methane combustion [29]. Consequently, if the PdO content in the catalyst increases, then the activity also increases.

During cooling, the reoxidation peak appeared at the same temperature, independent of the duration of preoxidation. However, the sample that was preoxidised for 10 h had a slightly larger reoxidation peak, whereas the as-prepared sample had the smallest peak. Nonetheless, the reoxidation peak during cooling appeared at a lower temperature than for Pd/Al_2O_3.

The reoxidation coefficients were also determined for this catalyst and are given in Table 2. All δ values for $PdPt/Al_2O_3$ were clearly >1 and in most cases increased with the duration of preoxidation. Again, this is related mostly to the increasing reduction peak and less to the changes in the reoxidation peak. This result reflects a slow reoxidation process that did not reach completion before the decomposition peak.

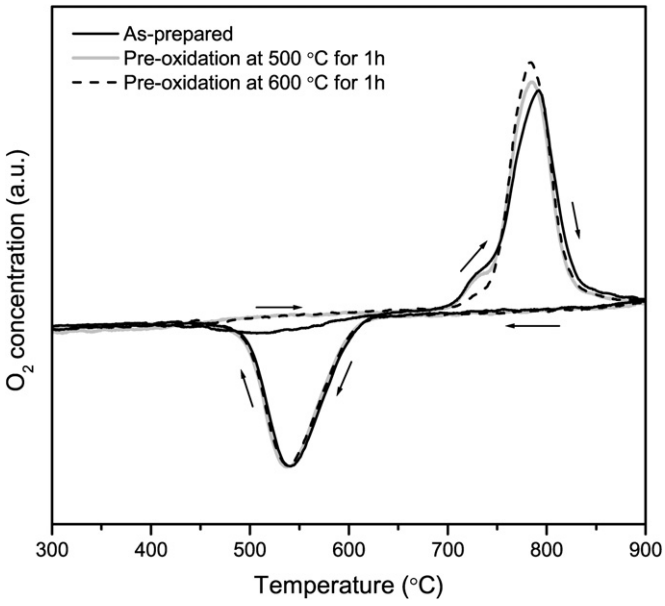

Fig. 5. TPO profiles of Pd/Al_2O_3. The sample was either as-prepared or preoxidised at various temperatures.

3.3. Oxidation at various temperatures

3.3.1. The Pd/Al_2O_3 catalyst

To investigate the influence of temperature on the catalysts, the samples were preoxidised at various temperatures for 1 h before the second TPO cycle. The TPO profiles of Pd/Al_2O_3 are presented in Fig. 5. Preoxidation at 500 and 600 °C minimised oxygen uptake between 450 and 630 °C for the as-prepared sample during heating.

Small variations of the PdO decomposition peaks were observed for the various temperatures. The sample preoxidised at 600 °C showed a slightly lower intensity of the first peak, but the second peak was somewhat higher than that for the sample preoxidised at 500 °C. This indicates that both temperature and duration of preoxidation affect the decomposition peaks.

The total area of the PdO decomposition peaks increased slightly with preoxidation temperature, indicating that more PdO was formed at 600 °C than at 500 °C. Despite the higher PdO concentration, a greater drop in activity occurred at the higher temperatures (see Fig. 1). Therefore, a decreasing amount of PdO most likely was not the reason for the loss of activity.

The reoxidation peaks during cooling were similar for the various preoxidation temperatures. This result indicates that once the catalyst is reduced, the material obtains the same morphology independent of the pretreatment.

The reoxidation coefficients of Pd/Al_2O_3 are compiled in Table 3 for the various temperatures; all values are >1. The δ value of the sample preoxidised at 600 °C is greater than that of the sample preoxidised at 500 °C, likely associated with the higher decomposition peaks.

To gain insight into the behaviour of Pd/Al_2O_3 in the TPO experiments, samples were cooled in helium to ambient temperature at different stages during experiments. Thereafter, the samples were studied ex situ by PXRD and TEM/EDS. Four

Table 3
The reoxidation coefficient δ of the samples that were preoxidised for 1 h at different temperatures

Sample	As-prepared	400 °C	500 °C	600 °C	655 °C	665 °C	800 °C
Pd/Al_2O_3	1.33	–	1.37	1.39	–	–	–
$PdPt/Al_2O_3$	2.43	2.32	3.07	3.68	3.06	2.89	2.56

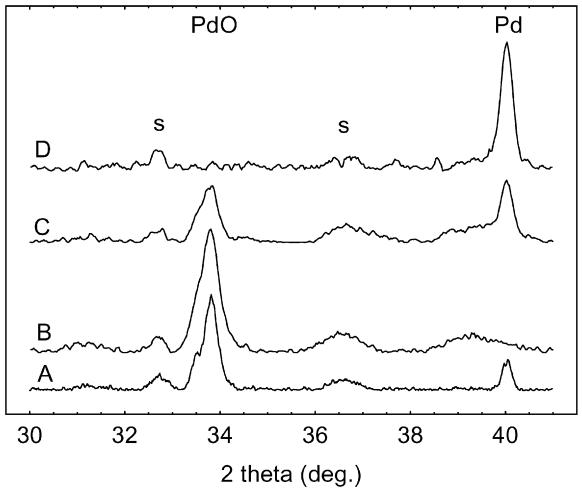

Fig. 6. PXRD patterns of Pd/Al_2O_3 for (A) as-prepared, (B) preoxidation at 500 °C, (C) preoxidation at 775 °C, (D) preoxidation at 900 °C. Reflex from δ-Al_2O_3 is labelled as S.

different samples were selected. The first sample was the as-prepared catalyst. The second sample was preoxidised for 10 h at 500 °C, the same temperature as in the activity test. The third sample was treated in the same way as the second sample before heating to 775 °C, a temperature at which the PdO decomposition started but did not reach completion. The last sample was taken after 5 min at 900 °C, when decomposition was completed.

The results of the PXRD analyses are presented in Fig. 6. All samples were supported on δ-Al_2O_3. The as-prepared sample consisted mostly of PdO ($2\theta = 33.8°$), but small amounts of metallic Pd ($2\theta = 40.1°$) were also detected. When the material was preoxidised at 500 °C, the peak indicating metallic palladium vanished along with an increase in the PdO reflection, demonstrating that the sample was somewhat more oxidised. When the temperature was raised to 775 °C, PdO decomposition started but was not completed, as demonstrated by reflections from both PdO and Pd. In the sample obtained at 900 °C, only metallic palladium was detected. The PXRD outcome is well in agreement with the TPO results. Furthermore, a sample taken from the monolith after the 12 h-activity test had a similar PXRD pattern (not shown in figure) as the sample preoxidised at 500 °C, confirming that the preoxidation procedure is representative of the used material.

Images from the morphological study by TEM/EDS of the four samples are presented in Figs. 7a–7e. The analyses reveal that all samples have well-distributed palladium-containing particles on the alumina surface in the range of 30–100 nm. According to the element analyses, the palladium particles are the darker spots, whereas the alumina support is shown as the light-gray areas.

Fig. 7a shows a representative palladium particle of the as-prepared sample. As shown in the figure, the centre of the particle is darker than the external parts. From the PXRD results, it can be concluded that both PdO and Pd are present in the as-prepared material. Thus, the darker parts of the particle shown in the TEM image are most likely metallic palladium (as an effect of denser material), whereas the lighter parts presumably consist of PdO. Hence, the palladium-containing particles appear to be not fully oxidised, but rather to consist of a mixture of both Pd and PdO domains. Even though PdO is the thermally favoured phase at this temperature range, Ciuparu et al. [7] reported that metallic Pd and PdO may coexist in a catalyst for extended periods due to a slow oxidation process.

The lack of facetted crystals indicates that the particles in the as-prepared material were composed of smaller (5–10 nm), randomly oriented crystals. At the outer surface of the particle, patches of smaller (3–5 nm) crystals are seen. According to the elemental analyses, these particles consist of palladium, but the oxidation state of the palladium cannot be determined using EDS. In addition, the particle size likely is too small to be detected by PXRD. Due to the polycrystalline PdO particles around the areas of Pd metal, the description of this structure is inconsistent with the core–shell model, which is supposed to have uniform layers of PdO around the Pd metal.

The oxidation mechanism of Pd is not very clear, and various ideas on how it occurs have been proposed. Lyubovsky et al. [30] observed by TEM rough polycrystalline PdO particles on reoxidation by cooling the sample after thermal decomposition. Based on this result, they excluded the possibility of a process involving growth of a surface oxide on a shrinking metal core. This idea appears to be consistent with the findings presented in this paper. Because the as-prepared catalyst was calcined at 1000 °C (a temperature above the thermal stability of PdO), the observed morphology is most likely due to this phenomenon of reoxidation, resulting in polycrystalline particles with mixtures of small PdO and Pd crystals.

The morphology changed after the catalyst was preoxidised at 500 °C. A considerable amount of the particles became fully oxidised, and some appeared to have a more crystalline structure. Fig. 7b shows an image of a representative palladium particle; the internal structure is composed of single crystals that overlap each other and form moire fringes with a rougher material on the outside surface. The inner part is most likely due to the small crystals, shown in the as-prepared material, having agglomerated into a larger crystal. In other cases, the particles appear to be built up of small PdO domains, as shown in Fig. 7c.

According to Ho et al. [31], the uptake of oxygen for Pd is very slow at ambient temperature and it remains adsorbed on the surface of the Pd crystals without further penetration into the bulk. Bulk oxidation into PdO becomes pronounced only above 500 °C. Hence, when storing the incompletely oxidised as-prepared sample at ambient temperature, insignificant amounts of PdO will be formed. When the temperature is in-

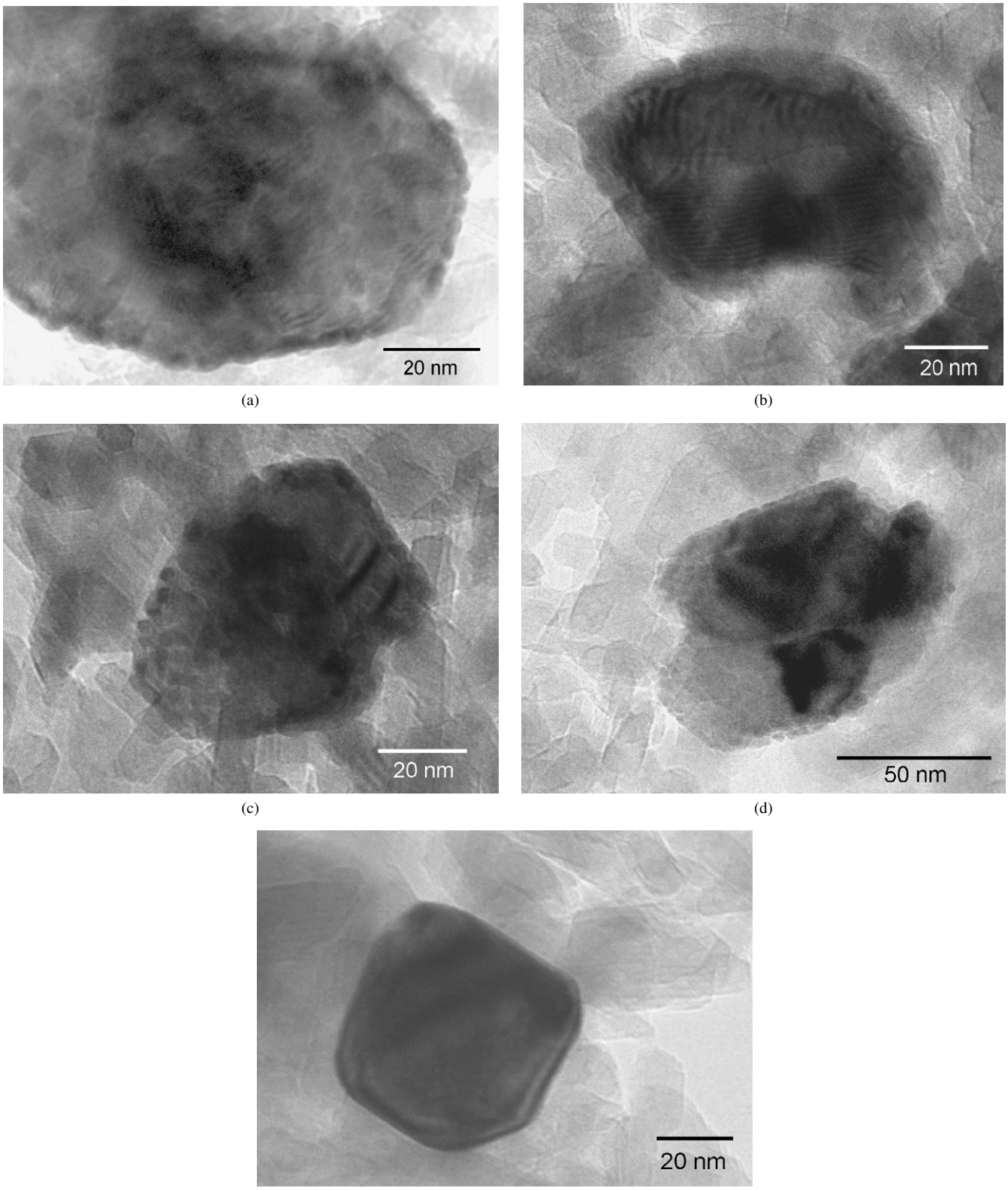

Fig. 7. TEM images of the Pd/Al_2O_3 catalyst. (a) As-prepared, (b, c) preoxidised at 500 °C for 10 h, (d) preoxidised at 500 °C for 10 h followed by further heating up to 775 °C where PdO decomposition has started but is incomplete and (e) heated up to 900 °C where PdO decomposition is completed.

creased to 500 °C, as was the case for the preoxidised samples, the oxidation will proceed further. The small crystals observed in the as-prepared material are likely to reach full oxidation and agglomerate into larger particles, resulting in fewer grain boundaries. This may perhaps be one of the explanations of the gradually decreasing activity.

Lyubovsky et al. [32] have reported an increase in the activity after treating the catalyst above the thermal decomposition temperature. They suggest that this phenomenon results from the rougher surface formed on reoxidation being more active than the fully oxidised catalyst. This is consistent with the results presented in this paper, because the as-prepared catalyst has polycrystalline morphology. During reaction, however, the oxidation of the catalyst is most likely proceeding further, as all characterisation techniques used in this study indicate, losing active surface and thereby activity.

According to Carstens et al. [33], the activity for methane combustion may be enhanced by producing small amounts of metallic Pd on the surface of PdO. Pd is more effective in dissociatively adsorbing methane, which normally is a difficult molecule to split. The fragments of the methane molecules are then rapidly diffused to the Pd–PdO interface, where reduction of the palladium oxide occurs. Increasing the degree of oxidation of the sample, which properly takes place during reaction, decreases the number of Pd–PdO interfaces, possibly causing a decline in activity. However, the extent of the effects of oxidation and crystal growth on catalytic activity is difficult to quantify; other deactivation processes may occur simultaneously.

Another feature of the small crystals of metallic palladium is that they can act as nucleation spots for the decomposition of PdO, when Pd crystals are in boundary contact with PdO crystals. This may be the cause of the first decomposition peaks in the TPO experiments. If this is the case, then the amount of metallic Pd in a sample reflects the size of the first peak in a TPO experiment. This is in line with the first peak in the TPO profile of the preoxidised samples being smaller, because the sample contains less metallic Pd.

After a TPO experiment has reached 775 °C, the decomposition of PdO into Pd is halfway completed. From TEM investigations the material exhibits individual palladium particles that are completely or partly reduced, but also some particles that appear to be unaffected. The partly reduced particles reveal that the transformation starts with a nucleation of Pd on the PdO crystals (see Fig. 7d). As the reduction progresses, the metallic palladium nucleates and grows on each crystal, forming a number of crystals. By heat treatment at 900 °C, these may form a single crystal with time. This structure with partly reduced particles during the thermal reduction of PdO is similar to that observed by Datye et al. [34], who found only metallic Pd on the surface of the PdO crystal. In contrast, Voogt et al. [35] suggested a structure consisting of a metallic core with an oxide skin. The former appears to be more in line with the findings of the present paper.

A typical TEM image of the sample treated at 900 °C is presented in Fig. 7e. The particles in this sample are well facetted, indicating that they consist of larger crystals. According to the PXRD result of the sample heated to 900 °C, the particles presumably consist of metallic palladium. Chen et al. [36] have observed a similar morphology of a thermally reduced palladium catalyst.

3.3.2. *The PdPt/Al_2O_3 catalyst*

Preoxidation of PdPt/Al_2O_3 was also studied by TPO at various temperatures, as shown in Fig. 8. The intensity of the decomposition peak during heating was clearly affected by the preoxidation temperature. The preoxidation at 400 °C gave only a small increase in the peak intensity compared to the as-prepared sample. When the temperature was increased to 500 °C, the decomposition peak became considerably larger, but the largest peak after preoxidation for 1 h was obtained for the sample preoxidised at 600 °C. The sample preoxidised at 800 °C showed any increase in the peak intensity, similar to the as-prepared sample. Hence, PdO formation with time is possible only below the temperature of decomposition.

The significant variation of the reduction peak with preoxidation temperature suggests that more PdO was formed at 600 °C than at 500 °C, which would explain the larger increase of methane conversion with time at the higher temperatures (see Fig. 2). However, preoxidation at temperatures above the decomposition of PdO are not favourable for PdO formation and thus also not for activity.

The reoxidation coefficients of PdPt/Al_2O_3 are shown in Table 3 for the various temperatures. A larger variation is seen for PdPt/Al_2O_3 than for Pd/Al_2O_3, due mostly to the size of the reduction peak and less to the reoxidation peak. During cooling, the reoxidation peaks were almost equal for the various temperatures. Thus, the bimetallic sample formed more PdO during heating compared with the monometallic sample.

By preoxidising the catalyst at a temperature on the decomposition peak, a double peak was obtained, as shown in Fig. 9. When preoxidation was carried out at 655 °C, the first peak was smaller and appeared at 659 °C, whereas the second peak was considerably larger and appeared at 676 °C. The reverse behaviour occurred for the sample preoxidised at 665 °C, where the first peak was larger than the second peak. For both sam-

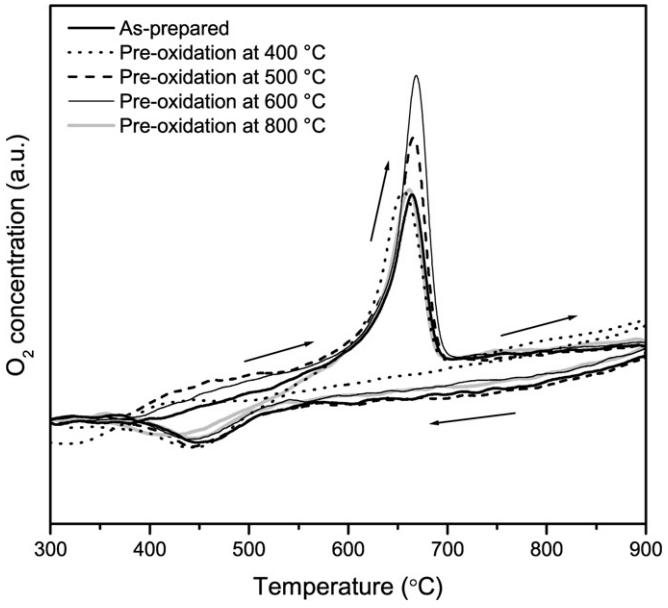

Fig. 8. TPO profiles of PdPt/Al_2O_3. The sample was either as-prepared or preoxidised at various temperatures.

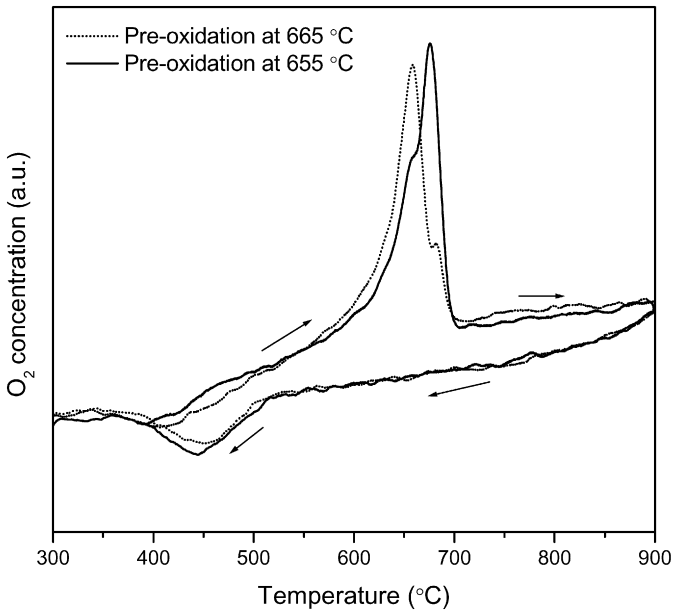

Fig. 9. Temperature-programmed oxidation plots of $PdPt/Al_2O_3$. The sample was preoxidised at temperatures on the reduction peak, i.e. 655 and 665 °C.

ples, the total area of the peaks was somewhat larger than the peak area of the sample that was not preoxidised, indicating that some PdO formed during the treatment. This is probably related to how far the decomposition has proceeded during the heat treatment and how rapidly reoxidation is occurring during cooling. However, further investigation is required to determine the cause of the double peak.

To investigate the nature of the $PdPt/Al_2O_3$ at various temperatures in the TPO experiments, the samples were cooled in helium to ambient temperature. Preoxidation was carried out for 10 h for all temperatures before further ex situ analyses. In the PXRD diffraction patterns of these samples, δ-Al_2O_3, PdO and Pd–Pt alloys were the only crystal phases observed. The as-prepared sample had a PdO peak at $2\theta = 33.8°$ and a metallic phase between the 2θ values of metallic Pd and Pt at 81.3° and 82.2°, respectively. The PdO(101) peaks are shown in Fig. 10a. The sample preoxidised at 500 °C shows a diffraction pattern similar to that of the as-prepared sample, but the PdO reflection is considerably larger. At 655 °C, the temperature reached the reduction peak in the TPO experiment, and the amount of PdO in the sample was smaller, indicating that the decomposition of PdO had started but had not reached completion. For the sample obtained at 800 °C, the PdO peak vanished. A sample obtained from the monolith after the 12 h-activity test was evaluated by PXRD and exhibited a diffraction pattern similar to, but slightly more oxidised than, that of the sample taken at 500 °C.

The changes in PXRD with the various temperatures for the metallic peaks are shown in Fig. 10b. Calculating the solid solution composition, Pt_xPd_{1-x}, revealed that the x value changed with temperature. The solid solution of the as-prepared sample had a value of $x = 0.43$, whereas the solid solution of the sample obtained at 500 °C had a value of $x = 0.48$. Consequently, by preoxidising the sample below the temperature of PdO decomposition, the material obtained a solid solution

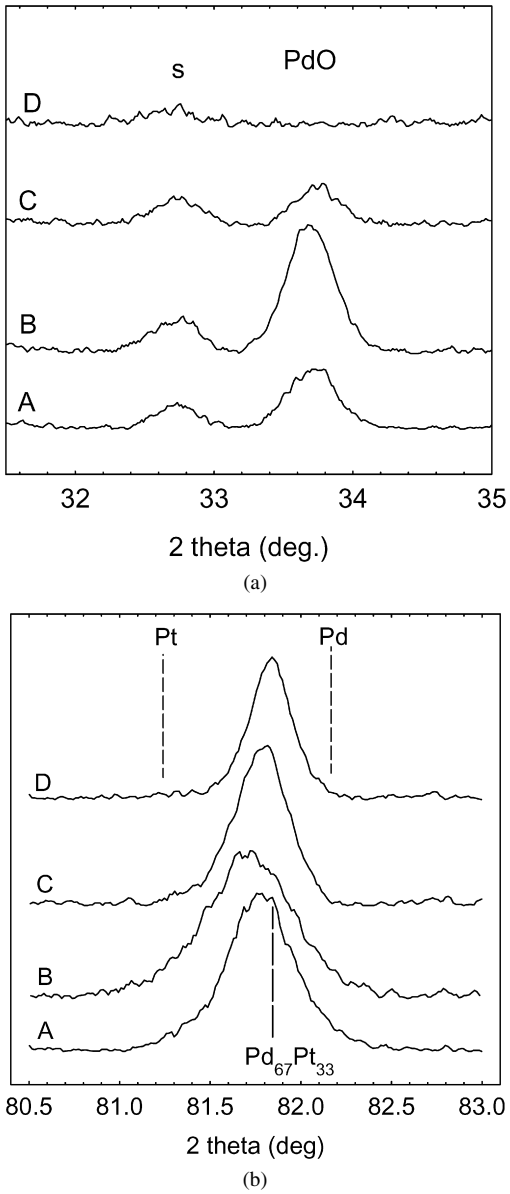

Fig. 10. PXRD patterns of the $PdPt/Al_2O_3$ catalyst for the (a) (101) reflex of PdO (b) (311) reflex of Pt_xPd_{1-x} alloy, in as-prepared (A), preoxidised at 500 °C (B), preoxidised at 655 °C (C) and preoxidised at 800 °C (D). Reflex from δ-Al_2O_3 is labelled as S.

closer to $x = 0.5$. This is the most likely reason for the ability of $PdPt/Al_2O_3$ to form PdO during reaction. Pd is dissolved out from the solid solution, and because PdO is the stable phase, under these conditions, the metallic Pd will oxidise into PdO. Note, however, that PdO formation appears to be a finite process and probably does not exceed $x = 0.5$. This is in line with the conversion levelling out after 12 h in the activity test, as well as with the increase of the reduction peak shown in the TPO profiles becoming smaller with time. Accordingly, the palladium and platinum in the catalyst will not end up in two separate particles.

The solid solution of the sample taken at 800 °C had a composition close to the nominal value of the catalyst, that is, $x = 0.33$. This indicates that once PdO decomposed, the metal-

lic palladium was incorporated into the solid solution. When the catalyst is reoxidising, Pd must diffuse out from the solid solution to become oxidised, which may explain the slow reoxidation for $PdPt/Al_2O_3$. However, this activation process most likely will occur only after the catalyst is treated under conditions favourable for PdO decomposition. If the catalyst is operating below the decomposition point of PdO, then the activity will most likely stagnate after a while and remain constant.

To further investigate the catalyst, the preoxidised samples were studied by TEM and EDS. The as-prepared sample contains 30–50 nm noble metal particles, with almost constant composition. The particles are well distributed and separated in the alumina support. Each particle was divided into two parts; EDS measurements confirmed that one part was rich in Pd and the other part contained both Pd and Pt, thus corresponding to PdO and Pt_xPd_{1-x} alloy, respectively.

No evidence of metallic Pd was found in the Pd-rich part, signifying that this domain consists of only PdO with no contribution of Pd. The mixed palladium phase (PdO and Pd), which is claimed to be the more active structure for methane conversion [32,33], was present in the as-prepared Pd/Al_2O_3 catalyst. As discussed previously, during the course of the experiment, the structure in the monometallic catalyst changed as the metallic Pd became oxidised, likely causing a decline of activity. In the case of the bimetallic catalyst, the metallic Pd appeared to be absent in the PdO part. Thus, less reconstruction of the PdO part occurred during operation, possibly resulting in less changes in activity and higher stability of methane conversion. The process of ejecting Pd out from the alloy will result only in increased PdO. Furthermore, due to the close contact with the alloy, the PdO part in $PdPt/Al_2O_3$ will always have a metallic source, which possibly will aid in splitting of the methane molecules. This may be one reason for the greater activity after 6.6 h, despite the lower palladium concentration in the $PdPt/Al_2O_3$ compared with Pd/Al_2O_3.

Fig. 11a shows a representative image of the material after preoxidation at 500 °C. The particle has a morphology similar to that of the as-prepared sample, but with a larger Pd-rich part. The alloy exhibited facetted surfaces, whereas corrosion was found on the interface with the oxide. The image also shows that the oxide surfaces contained 2–3 nm particles, similar to the monometallic palladium material.

At 800 °C, only well facetted Pt_xPd_{1-x} particles were found (see Fig. 11b). According to the EDS analysis, Pd and Pt were evenly spread in the noble metal particles. Palladium was never found without platinum.

3.3.3. Surface chemistry

The surface chemistry of as-prepared Pd and Pd–Pt catalysts was previously investigated by XPS [29]. The monometallic palladium catalyst showed a binding energy of 337.1 eV for $Pd3d_{5/2}$. The literature reports that this value is slightly too high for pure PdO (Pd^{2+}, 336.7 eV [37,38]), indicating the possibility of a mixture with Pd^{4+} (337.5 eV [39,40]). Pd^{4+} (PdO_2) is generally known to be highly unstable, but according to Moroseac et al. [41], metal–support interactions may stabilise this species. For the bimetallic Pd–Pt catalyst, the $Pd3d_{5/2}$ band

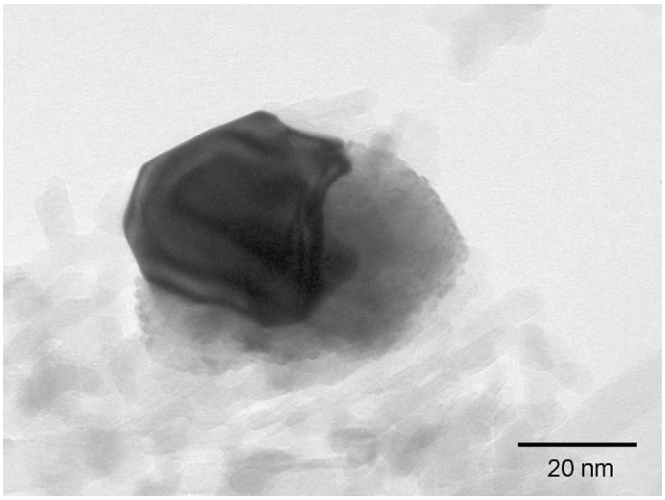

(a)

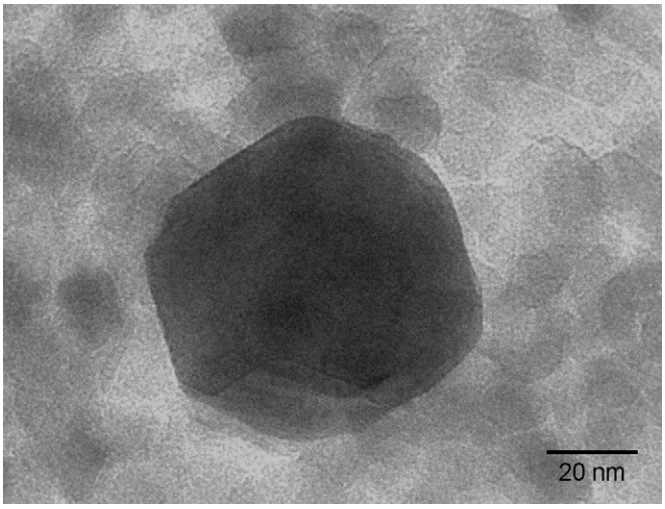

(b)

Fig. 11. TEM images of Pt_xPd_{1-x}/PdO particles in the $PdPt/Al_2O_3$ catalyst after (a) pre-oxidation at 500 °C for 10 h, (b) pre-oxidation at 800 °C for 10 h.

was divided into two different components: one at 336.0 eV attributable to Pd^{2+} and one at 337.3 eV attributable to Pd^{4+}. In this case, the energy of the Pd^{2+} component was slightly too low compared with the values reported in the literature, indicating the possibility that Pd^0 may also be on the surface of the as-prepared bimetallic Pd–Pt catalyst, which was not assumed to be the case at the time of this study. Platinum was also observed in two oxidation states (Pt^0 and Pt^{4+}) with band maxima at 314.4 and 317.0 eV, respectively.

This study has investigated how the XPS spectra of the Pd3d band vary with preoxidation of the $PdPt/Al_2O_3$ catalyst. By assuming that all three oxidation states (Pd^0, Pd^{2+}, and Pd^{4+}) may be present on the catalyst surfaces, the amount of each state was determined by convolution using binding energies from the literature (335.2 eV [42,43], 336.7 eV [37,38], and 337.5 eV [39,40], respectively). The spectra are shown in Fig. 12, and the binding energies and the oxidation states of Pd are compiled in Table 4.

In the as-prepared sample, all oxidation states were observed, dominated by Pd^0 and Pd^{2+}. Pd^{4+} is most likely present

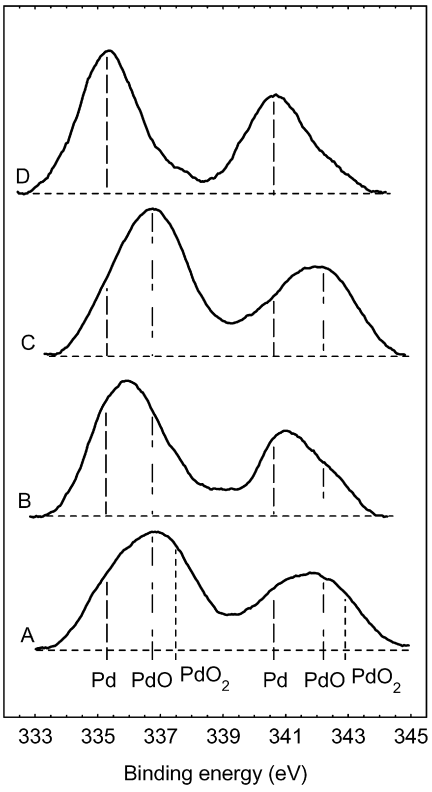

Fig. 12. Pd 3d core level spectra recorded by XPS on PdPt/Al_2O_3 catalyst of as-prepared (A), Ar-etched (B), preoxidised at 500 °C (C) and preoxidised at 800 °C (D).

Table 4
Binding energies of core electrons determined from XPS spectra of the different catalyst materials

Catalyst	$Pd3d_{5/2}$ (eV)	Oxidation state	Relative intensity (%)
5 wt% Pd/Al_2O_3 [a]	337.1		100
2:1 PdPt/Al_2O_3 [a]	336.0		22
	337.3		78
PdPt/Al_2O_3 as-prepared	335.2	Pd^0	38
	336.7	Pd^{2+}	47
	337.5	Pd^{4+}	15
PdPt/Al_2O_3 Ar-etched	335.2	Pd^0	71
	336.7	Pd^{2+}	29
	337.5	Pd^{4+}	0
PdPt/Al_2O_3 at 500 °C	335.2	Pd^0	17
	336.7	Pd^{2+}	83
	337.5	Pd^{4+}	0
PdPt/Al_2O_3 at 800 °C	335.2	Pd^0	100
	336.7	Pd^{2+}	0
	337.5	Pd^{4+}	0

[a] Previous investigation, see paper by Persson et al. [29].

only on the surface of the catalyst, because no Pd^{4+} was detected in the bulk phase by PXRD. To investigate whether this in fact is the case, depth profiling by argon etching was carried out. As expected, after the etching of the material, Pd^{4+} disappeared, and the oxidation states of the bulk materials consisted of Pd^{2+} and Pd^0. Because the amount of Pd^0 is fairly high in this sample, it is possible that some of the PdO phase also was reduced during etching.

By oxidising the sample for 10 h at 500 °C, the intensity of the Pd^0 peak decreased along with an increase in the Pd^{2+} peak. This demonstrates that more PdO was present at the surface of the sample compared to the as-prepared sample, similar to the bulk composition observed by PXRD. The low fraction of metallic palladium suggests that even the Pd–Pt alloy was oxidised on the surface to some extent.

No Pd^{4+} was detected in the sample treated at 500 °C; thus, it likely was not present during the combustion reaction. This finding is not surprising, because Pd^{4+} is well known to have low stability at higher temperatures. After heating at 800 °C, only the metallic form of palladium was present on the surfaces of the alloyed particles.

3.4. Thermal aging

The catalysts were aged at 1000 °C for 10 h in an air stream with 15 vol% of steam. This is a very harsh aging, because the temperature is above the normal operation temperature of the catalysts and above the temperature window of PdO. However, these conditions will speed up the aging and give an indication of the long-term stability of the catalysts. The monoliths and the catalyst powders were aged at the same time so as to facilitate evaluation of the activity and characterization of the samples.

Fig. 13 shows the activities of as-prepared and aged Pd/Al_2O_3 catalysts. The aged catalyst had considerably lower activity than the as-prepared catalyst, where the largest losses occurred at the third and forth temperature steps. The activity decreased with time for both samples, although that of the aged sample decreased less.

Fig. 14 shows the activities of the as-prepared and aged PdPt/Al_2O_3. The loss of activity due to thermal aging was significantly less than that for the monometallic Pd catalyst. No difference is observed between the combustion profiles of the aged and the as-prepared catalysts for the two final temperature steps at 720 and 770 °C. For the other temperature steps, small variations are seen. Nevertheless, the ability to maintain a constant activity is sustained on aging.

The loss of activity at temperatures above 670 °C is most likely related to the PdO decomposition, because the TPO experiments showed PdO decomposition in this temperature range. However, the TPO decomposition started already at 625 °C. The lower decomposition temperature is probably related to the fourfold lower partial pressure of oxygen used in the TPO experiments compared with the activity test. The decomposition temperature of PdO was strongly influenced by the partial pressure of oxygen, and the decomposition temperature increased with increasing pressure [44,45].

The values of BET surface areas, crystal sizes, and noble metal loadings of the samples are compiled in Table 1. The drop of surface area with aging may decrease the activity of both catalysts to some extent. But because the drop is in the same range for the two catalysts, the differences in activity loss are most likely not associated with the different surface areas. TEM studies of the aged materials (not shown in any figure) revealed that the particle size of the alumina was larger than that in the as-prepared samples. According to the literature,

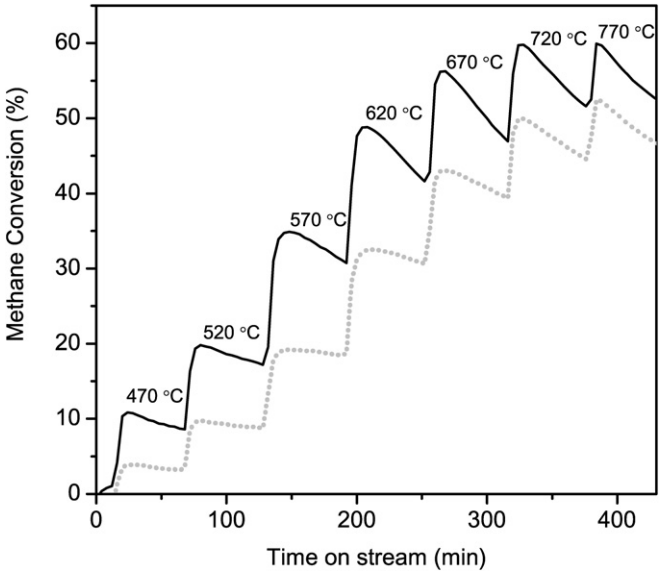

Fig. 13. Steady-state activity tests of Pd/Al_2O_3; methane conversion as a function of time on stream. The black line represents the activity of the as-prepared sample and the gray dotted line represents the activity of the aged sample.

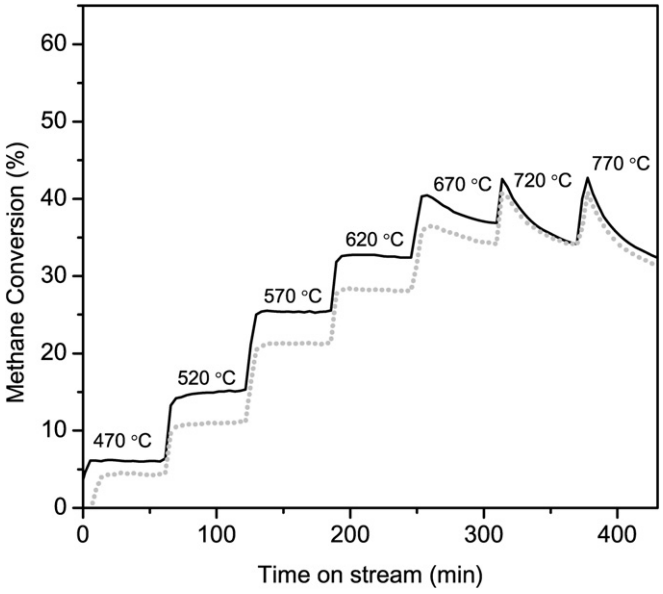

Fig. 14. Steady-state activity tests of $PdPt/Al_2O_3$. Methane conversion as a function of time on stream. The black line represents the activity of the as-prepared sample and the gray dotted line represents the activity of the aged sample.

the transformation into θ-Al_2O_3 occurred at 1050 °C [46] and thus is likely to occur during natural aging. This transformation will slightly decrease the surface area and thereby decrease the activity. The PXRD diffraction patterns confirm the higher content of θ-Al_2O_3 in the aged samples compared with the as-prepared samples. Nonetheless, high amounts of the δ-Al_2O_3 phase were present in the aged sample; α-Al_2O_3 was not detected even in the aged samples.

As shown in Table 1, the increase in the average crystal size of PdO determined from the PXRD data was similar for the two catalysts as well. Thus, the greater activity loss of Pd/Al_2O_3 with aging may not be attributed to increasing crystal size, but rather may be an effect of Pd being encapsulated into a surface coating layer of PdO over the metal, preventing good contact with both Pd and PdO surfaces. Furthermore, the increase in crystal size was very small with aging and may be within the experimental error.

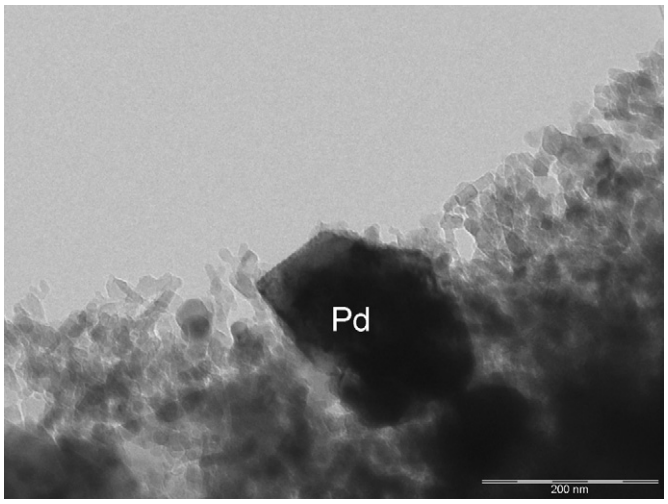

Fig. 15. TEM image of Pd/Al_2O_3 sample, aged at 1000 °C, 15 vol% steam for 10 h.

The catalyst in the present study was calcined at considerably higher temperature than that used in most aging studies, resulting in larger initial sizes of the palladium-containing particles. Due to the larger palladium particles, and thus the larger distance between them, the ability to move in the alumina matrix to obtain growing and sintering was reduced. Nevertheless, the smaller crystals might migrate through the alumina material.

Gélin et al. [1] have shown that alumina-supported Pt catalysts are less resistant to thermal aging in steam at 600 °C than Pd catalysts. The dispersion of Pt on the alumina decreased significantly, resulting in lower activity. In contrast to monometallic Pt catalysts, the alloyed Pd–Pt system showed significant stabilisation against sintering [47]. This appears to also be the case for the catalysts presented in this paper, for which only small changes in the alloy crystal size were observed.

Vaporisation of the noble metals also may decrease the activity. According to the literature, Pt is more easily vaporised than Pd, but the combination of the two make the platinum more resistant against vaporisation [48]. Table 1 shows that the noble metal loading was slightly decreased for both catalysts after aging. For the Pd/Al_2O_3 catalyst, the Pd loading was decreased from 5.1 to 4.8 wt%. In $PdPt/Al_2O_3$, the Pd content remained constant, and only the platinum content decreased. Because palladium in the form of PdO appears to be the active phase in the bimetallic catalysts, the loss in Pt probably will not decrease the activity severely. It is interesting to note that the alloy appeared to stabilise the Pd phase, probably related to the solid solution formation at higher temperatures having the nominal composition value.

A representative TEM image of the aged Pd/Al_2O_3 materials is presented in Fig. 15. The particles have more facetted

structures, and almost no metallic Pd is found in the sample. Similar morphology was found in the preoxidised sample, as discussed previously. Thus, the reconstruction into a less active morphology may be one explanation for the poor stability against thermal aging.

According to TEM analyses of the aged $PdPt/Al_2O_3$ sample, the alloy part is unaffected by aging, although the PdO part is larger. That the oxidation proceeded during aging is also indicated by the x-values determined from PXRD; for the as-prepared sample, $x = 0.43$, but this increased to $x = 0.46$ after aging. However, the increase in the x-value also may be due to the lower amount of Pt in the sample after aging.

In summary, thermal aging achieved a structure similar to that after preoxidation at 500 °C; that is, the metallic Pd in Pd/Al_2O_3 oxidised into PdO at the same time as the crystals grew, whereas $PdPt/Al_2O_3$ maintained the two-domain structure in which the PdO part became larger and the alloy obtained a structure closer to $x = 0.5$. Thus, Pd/Al_2O_3 acquired a less active structure over time, whereas $PdPt/Al_2O_3$ achieved a more active structure. However, thermal aging also causes other phenomena that may result in a drop in activity for both catalysts, such as decreased surface area and vaporisation of noble metals. This feature will probably be less pronounced at the normal operation temperature of the catalysts, because they were not observed for the preoxidised sample.

4. Conclusions

Our study of the stability of methane conversion over Pd/Al_2O_3 and $PdPt/Al_2O_3$, as well as the corresponding morphologies, has led to the following conclusions:

- The activity over $PdPt/Al_2O_3$ was greater than that over Pd/Al_2O_3 after 6.6 h for the conditions used in this study.
- The activity over Pd/Al_2O_3 dropped significantly with time, and the loss was larger at higher temperatures. Because slightly more PdO was formed during operation in oxidising atmosphere, this activity drop most likely cannot be attributed to loss of Pd.
- The as-prepared Pd/Al_2O_3 catalyst was incompletely oxidised initially, but formed more PdO during operation. The palladium-containing particles were composed of polycrystalline domains of both PdO and Pd randomly oriented inside the particles. Preoxidising the sample at 500 or 600 °C changed the morphology of the particles into larger crystals and caused the sample to become fully oxidised. The decline in activity may be due to this reconstruction. By treating the catalyst at a temperature above that of thermal PdO decomposition, the structure of the as-prepared sample likely can be recovered.
- The thermal decomposition of PdO was initiated by creating one or two nuclei of Pd on each PdO crystal. The completely reduced sample consisted of large facetted crystals.
- The activity of $PdPt/Al_2O_3$ increased with time. Results from TPO, XRD, XPS, and TEM indicate that the increase was due to significantly greater PdO production during operation. By increasing the oxidation temperature, more PdO was formed and stabilisation occurred more rapidly. However, the oxidation temperature must be below the PdO decomposition temperature for this to occur.
- The morphology of the noble metal particles in $PdPt/Al_2O_3$ consisted of two parts, one rich in PdO and the other consisting of an alloy between Pd and Pt. These two parts were always found in close contact. The alloy initially had a palladium-rich composition. During operation below the PdO decomposition temperature, the composition of the alloy changed toward a structure of equal molarity of Pd and Pt. The metallic palladium ejected from the solid solution was oxidised into PdO, which is more active for methane combustion, resulting in increased activity.
- On exposing $PdPt/Al_2O_3$ to higher temperature than allowed for PdO stability, the PdO decomposes and becomes incorporated into the solid solution between Pd and Pt. Hence, on cooling, the extra Pd in the solid solution must diffuse out from the solid solution to be oxidised back to PdO. This is probably the reason for the slow reoxidation process observed for the bimetallic catalyst.
- For the oxidation reaction of methane, stable conversion was observed only for the $PdPt/Al_2O_3$ catalyst, where both metallic Pd and PdO coexist on the surface, whereas for the Pd/Al_2O_3 catalyst, all Pd transformed into PdO over time.
- The thermal aging was worse for Pd/Al_2O_3 than for $PdPt/Al_2O_3$. Thus, Pt prevents the aging of Pd catalysts. The difference in aging may be attributed both to changes in the morphology and to the loss of palladium of the monometallic catalyst, which is not observed for the bimetallic catalyst.

Acknowledgments

This work was supported by the Swedish Energy Agency. The authors thank Sasol Germany GmbH for providing the alumina support. They also thank Professor Y. Teraoka and Dr. H. Kusaba at Kyushu University for helping with the XPS measurements.

References

[1] P. Gélin, L. Urfels, M. Primet, E. Tena, Catal. Today 83 (2003) 45.
[2] D.L. Mowery, M.S. Graboski, T.R. Ohno, R.L. McCormick, Appl. Catal. B 21 (1999) 157.
[3] J.K. Lampert, M.S. Kazi, R.J. Farrauto, Appl. Catal. B 14 (1997) 211.
[4] W.C. Pfefferle, J. Energy 2 (1978) 142.
[5] M.F.M. Zwinkels, S.G. Järås, P.G. Menon, T.A. Griffin, Catal. Rev. Sci. Eng. 35 (1993) 319.
[6] E.M. Johansson, D. Papadias, P.O. Thevenin, A.G. Ersson, R. Gabrielsson, P.G. Menon, P.H. Björnbom, S.G. Järås, in: J.J. Spivey (Ed.), in: Catalysis—Specialists Periodical Reports, vol. 14, Royal Soc. Chem., Cambridge, 1999, p. 183.
[7] D. Ciuparu, M.R. Lyubovsky, E. Altman, L.D. Pfefferle, A. Datye, Catal. Rev. 44 (2002) 593.
[8] K. Narui, H. Yata, K. Furuta, A. Nishida, Y. Kohtoku, T. Matsuzaki, Appl. Catal. A 179 (1999) 165.
[9] A. Ersson, H. Kušar, R. Carroni, T. Griffin, S. Järås, Catal. Today 83 (2003) 265.

[10] K. Persson, A. Ersson, A. Manrique Carrera, J. Jayasuriya, R. Fakhrai, T. Fransson, S. Järås, Catal. Today 100 (2005) 479.
[11] K. Persson, A. Ersson, K. Jansson, N. Iverlund, S. Järås, J. Catal. 231 (2005) 139.
[12] Y. Ozawa, Y. Tochihara, M. Nagai, S. Omi, Chem. Eng. Sci. 58 (2003) 671.
[13] D. Roth, P. Gélin, M. Primet, E. Tena, Appl. Catal. A 203 (2000) 37.
[14] Y. Ozawa, Y. Tochihara, A. Watanabe, M. Nagai, S. Omi, Appl. Catal. A 259 (2004) 1.
[15] K. Persson, A. Ersson, S. Colussi, A. Trovarelli, S.G. Järås, Appl. Catal. B 66 (2006) 175.
[16] H. Yamamoto, H. Uchida, Catal. Today 45 (1998) 147.
[17] K. Nomura, K. Noro, Y. Nakamura, Y. Yazawa, H. Yoshida, A. Satsuma, T. Hattori, Catal. Lett. 53 (1998) 167.
[18] C.L. Pieck, C.R. Vera, E.M. Peirotti, J.C. Yori, Appl. Catal. A 226 (2002) 281.
[19] K.E. Johansson, T. Palm, P.E. Werner, J. Phys. Sci. Instrum. 13 (1980) 1289.
[20] R.B. Anderson, K.C. Stein, J.J. Feenan, L.J.E. Hofer, Ind. Eng. Chem. 53 (1961) 809.
[21] P. Araya, S. Guerrero, J. Robertson, F.J. Garcia, Appl. Catal. A 283 (2005) 225.
[22] C.F. Cullis, T.G. Nevell, D.L. Trimm, J. Chem. Soc. Faraday Trans. 68 (1972) 1406.
[23] R. Burch, P.K. Loader, F.J. Urbano, Catal. Today 27 (1996) 243.
[24] G. Groppi, C. Cristiani, L. Lietti, P. Forzatti, in: A. Corma, F.V. Melo, S. Mendioroz, J.L.G. Fierro (Eds.), in: Stud. Surf. Sci. Catal., vol. 130, Elsevier Science, Amsterdam, 2000, p. 3801.
[25] G. Groppi, G. Artioli, C. Cristiani, L. Lietti, P. Forzatti, in: E. Inglesia, J.J. Spivey, T.H. Fleish (Eds.), in: Stud. Surf. Sci. Catal., vol. 136, Elsevier Science, Amsterdam, 2001, p. 345.
[26] R.J. Farrauto, M.C. Hobson, T. Kennelly, E.M. Waterman, Appl. Catal. A 81 (1992) 227.
[27] J.G. McCarty, Catal. Today 26 (1995) 283.
[28] R. Strobel, J. Grunwaldt, A. Camenzind, S.E. Pratsinis, A. Baiker, Catal. Lett. 104 (2005) 9.
[29] K. Persson, A. Ersson, K. Jansson, J.L.G. Fierro, S.G. Järås, J. Catal. 234 (2006) 14.
[30] M. Lyubovsky, L. Pfefferle, A. Datye, J. Bravo, T. Nelson, J. Catal. 187 (1999) 275.
[31] Y.S. Ho, C.B. Wang, C.T. Yeh, J. Mol. Catal. A Chem. 112 (1996) 287.
[32] M. Lyubovsky, L. Pfefferle, Appl. Catal. A 173 (1998) 107.
[33] J.N. Carstens, S.C. Su, A.T. Bell, J. Catal. 176 (1998) 136.
[34] A.K. Datye, J. Bravo, T.R. Nelson, P. Atanasova, M. Lyubovsky, L. Pfefferle, Appl. Catal. A 198 (2000) 179.
[35] E.H. Voogt, A.J.M. Mens, O.L.J. Gijzeman, J.W. Geus, Surf. Sci. 350 (1996) 21.
[36] J.J. Chen, E. Ruckenstein, J. Phys. Chem. 85 (1981) 1606.
[37] D.H. Kim, S.I. Woo, J.M. Lee, O. Yang, Catal. Lett. 70 (2000) 35.
[38] K. Otto, L.P. Haack, J.E. de Vries, Appl. Catal. B 1 (1992) 1.
[39] Y. Bi, G. Lu, Appl. Catal. B 41 (2003) 279.
[40] A.L. Guimarães, L.C. Dieguez, M. Schmal, J. Phys. Chem. B 107 (2003) 4311.
[41] M. Moroseac, T. Skála, K. Veltruská, V. Matolín, I. Matolínová, Surf. Sci. 566–568 (2004) 1118.
[42] R.J. Bird, P. Swift, J. Electron Spectrosc. Relat. Phenom. 21 (1980) 227.
[43] G. Johansson, J. Hedman, A. Berndtsson, M. Klasson, R. Nilsson, J. Electron Spectrosc. Relat. Phenom. 2 (1973) 295.
[44] W.E. Bell, R.E. Inyard, M. Tagami, J. Phys. Chem. 70 (1966) 3735.
[45] H. Zhang, J. Gromek, G.W. Fernando, S. Boorse, H.L. Marcus, J. Phase Equilib. 23 (2002) 246.
[46] C. Morterra, G. Magnacca, Catal. Today 27 (1996) 497.
[47] A. Morlang, U. Neuhausen, K.V. Klementiev, F.W. Schütze, G. Miehe, H. Fuess, E.S. Lox, Appl. Catal. B 60 (2005) 191.
[48] M. Chen, L.D. Schmidt, J. Catal. 56 (1979) 198.